Front. Energy 2015, 9(1): 31–42
DOI 10.1007/s11708-015-0347-9

RESEARCH ARTICLE

C. K. ARAVIND, G. SARAVANA ILANGO, C. NAGAMANI

A smooth co-ordination control for a hybrid autonomous power system (HAPS) with battery energy storage (BES)

Abstract The standalone hybrid power system constitutes a synchronous generator driven by a diesel engine, renewable energy source (wind) apart from a battery energy storage system. A coherent control strategy to regulate the voltage and frequency of the standalone grid is proposed in this paper. The system is simulated using Matlab/Simulink for preliminary validation and further tested on a laboratory prototype which involves a TMS320LF2407A DSP controller to digitally implement the control strategy. The dynamic behavior of the system is perused through the direct connection of an induction machine. The control strategy is verified for step changes in load and variation in wind power.

Keywords standalone hybrid power system, battery energy storage system (BESS), power conversion

1 Introduction

Main bulk power plants are displaced far from the load centers as per the current infrastructure in many of the countries. The largely interconnected network is used to transfer the electricity produced from such plants [1]. However, the extension of grid system to rural village areas with less population and thinly distributed lands is less feasible due to the economic constraints involved in constructing transmission lines [2,3]. A drift toward developing distributed energy generation which involves small-sized energy generation units located close to the consumers is developing [4]. Such types of standalone grid system are also being pursued by commercial and residential customers living in urban areas. A major component of such a standalone system is a diesel engine driven generator due to its dependability, ease of conveyance, installation and discontinuation [5]. Typically, the voltage distortion is high while starting induction motor loads or during load changes. Such issues can be related to the considerable source impedance of the generator [6]. Also, wet stacking caused by the partial burning of fuel, necessitates the operation of generator above 40% of its nominal power [7]. The significant advancement in power electronics technology over the past few decades has triggered the practice of integrating renewable sources like solar and wind into the standalone system [8–11]. However such integration mainly aims at minimizing the fuel consumption of the diesel generator by using the renewable sources to their fullest potential and not by replacing the diesel generator completely. The dithering of voltage and frequency is high because of the instantaneous changes in load as well as the variations in power supplied by the renewable energy sources which depend on natural resources [12–16].

Several topologies as well as control schema have been proposed and reported. Some works have concentrated on the operation of an energy storage system in the hybrid system. Compressed air storage and pumped energy storage have been utilized to compensate for the difference between generation and consumption [17–19]. The surplus electrical energy is stored in the form of kinetic energy. However, the drawbacks of such a system are that the spontaneous transfer of energy to electricity is not possible due to long-term energy storage management and it is not viable in all operating areas. The reliability of the standalone power system is ameliorated by using battery, a commonly found component where electricity storage is required [20–24]. However, it has several advantages: it is compliant to the hybrid system and battery storage based on power electronic systems and has a quick dynamic response. The battery has also been used to maintain the AC link voltage using power converters [20,25]. The AC

Received April 20, 2014; accepted August 10, 2014

C. K. ARAVIND, C. NAGAMANI
Department of Electrical and Electronics Engineering, National Institute of Technology, Tiruchirappalli 620015, India

G. SARAVANA ILANGO (✉)
Department of Electrical and Electronics Engineering, National Institute of Technology, Trichy 620015, India
E-mail: gsilango@nitt.edu

voltage of the generator output is rectified and supplied to DC link which is then inverted to supply the AC loads in such cases. A few researches have concerted their work on collaboration between the battery and other renewable sources [26–28].

This paper presents a smooth coordinated control strategy for the diesel generator and battery system to assist in regulating within set limit, the voltage and frequency of the standalone grid. Besides, the dynamic behavior of the diesel generator is perused and analyzed for step changes in loads. A detailed simulation study to analyze the efficacy of the control strategy as well as the overall system structure is made using Matlab/Simulink. Further, experiments are conducted on a laboratory prototype and the controller is digitally implemented on a TMS320LF2407A DSP controller. The results verify and validate the overall performance of the scheme.

2 System description

The block diagram of the standalone power system is depicted in Fig. 1. The system constitutes a diesel engine coupled to a synchronous generator (SG), battery energy storage system (BESS) with a bidirectional converter, renewable source (wind turbine coupled to squirrel cage induction generator (SCIG), critical and non-critical loads and dump load. The vital component that regulates the voltage magnitude and frequency of the standalone power system is the diesel generator. The speed of the diesel engine is maintained by using the governor control to vary the amount of fuel injected based on the load. The BESS plays a key role in absorbing as well as injecting power during dynamic conditions to stabilize the frequency and voltage and a dump load is used to prevent overcharging of the battery.

3 Mathematical modeling of standalone power system

The components in the standalone hybrid power system are mathematically modeled and explicated in this section.

3.1 Modeling of synchronous generator

The synchronous generator is modeled using the *d-q* model which disregards the reliance of the inductor on rotor position. The model must present the stator and rotor equations in relation to the rotor in order to coordinate with respect to the *d-q* axes. The synchronous generator voltage in *d-q* components can be expressed as

$$v_d = -R_s i_d - \omega\lambda_q - (L_{ls} + L_{md})\frac{di_d}{dt} + L_{md}\frac{di_{fd}}{dt}, \quad (1)$$

$$v_q = -R_s i_q - \omega\lambda_d - (L_{ls} + L_{mq})\frac{di_q}{dt}, \quad (2)$$

$$v_{fd} = R_{fd} i_{fd} - L_{md}\frac{di_d}{dt} + (L_{lfd} + L_{md})\frac{di_{fd}}{dt}, \quad (3)$$

where

$$\lambda_d = -(L_{ls} + L_{md})i_d + L_{md} i_{fd}, \quad (4)$$

$$\lambda_q = -(L_{ls} + L_{mq})i_q. \quad (5)$$

3.2 Modeling of bidirectional converter

The bidirectional converter is modeled using differential equations with respect to *d-q* components. Here, converter current is used as the state variable.

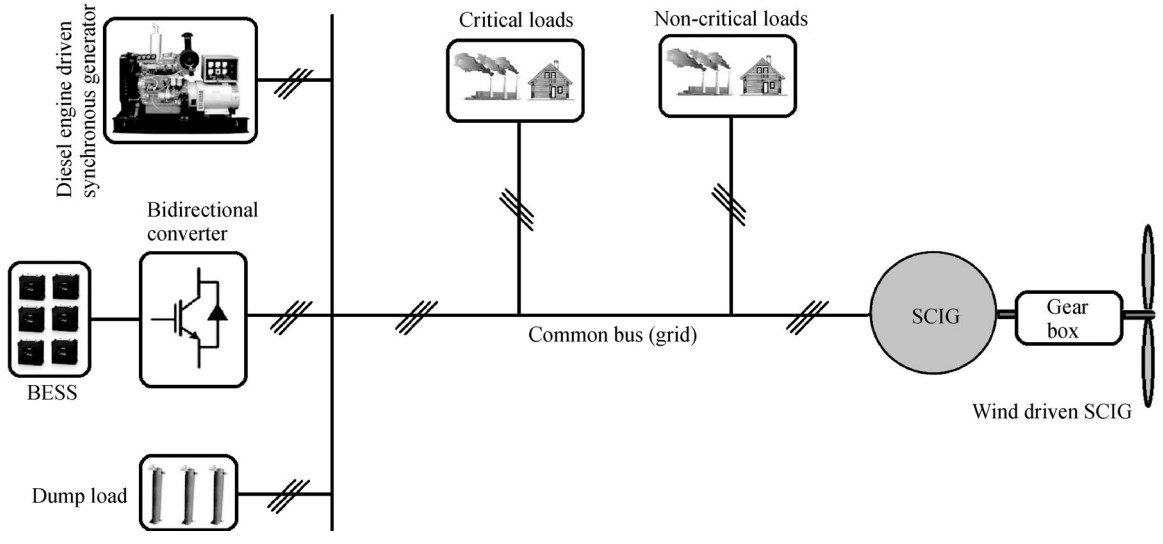

Fig. 1 Block diagram of proposed standalone power system

$$\frac{\mathrm{d}i_d}{\mathrm{d}t} = \frac{-r_{\mathrm{sh}}}{L_{\mathrm{sh}}} i_d + \omega i_q + \frac{1}{L_{\mathrm{sh}}}(V_{\mathrm{p}d} - V_{\mathrm{t}d}), \tag{6}$$

$$\frac{\mathrm{d}i_q}{\mathrm{d}t} = \frac{-r_{\mathrm{sh}}}{L_{\mathrm{sh}}} i_q - \omega i_d + \frac{1}{L_{\mathrm{sh}}}(V_{\mathrm{p}q} - V_{\mathrm{t}q}). \tag{7}$$

3.3 Modeling of induction generator

A grid excited, squirrel cage machine is considered as the grid connected induction generator. The machine is modeled using *d-q* components for dynamic analysis. The *d*-axis is aligned with the stator flux and *q*-axis is aligned with the stator voltage space vector. The differential equations that involve the stator and the rotor currents in the stator reference frame can be expressed as

$$L_{\mathrm{s}}\frac{\mathrm{d}i_{sq}}{\mathrm{d}t} = V_{sq} - R_{\mathrm{s}}i_{sq} - (\omega_{\mathrm{ms}})(L_{\mathrm{s}}i_{sd} + L_{\mathrm{o}}i_{rd}) - L_{\mathrm{o}}\frac{\mathrm{d}i_{\mathrm{r}q}}{\mathrm{d}t}, \tag{8}$$

$$L_{\mathrm{s}}\frac{\mathrm{d}i_{sd}}{\mathrm{d}t} = V_{sd} - R_{\mathrm{s}}i_{sd} - (\omega_{\mathrm{ms}})(L_{\mathrm{s}}i_{sq} + L_{\mathrm{o}}i_{\mathrm{r}q}) - L_{\mathrm{o}}\frac{\mathrm{d}i_{\mathrm{r}d}}{\mathrm{d}t}, \tag{9}$$

$$L_{\mathrm{r}}\frac{di_{rq}}{dt} = V_{\mathrm{r}q} - R_{\mathrm{r}}i_{\mathrm{r}q} + (\omega_{\mathrm{mr}} - \omega_e)(L_{\mathrm{r}}i_{\mathrm{r}d} + L_{\mathrm{o}}i_{sd}) - L_o\frac{\mathrm{d}i_{\mathrm{s}q}}{\mathrm{d}t}, \tag{10}$$

$$L_{\mathrm{r}}\frac{\mathrm{d}i_{\mathrm{r}d}}{\mathrm{d}t} = V_{\mathrm{r}d} - R_{\mathrm{r}}i_{\mathrm{r}d} + (\omega_{\mathrm{ms}} - \omega_{\mathrm{e}})(L_{\mathrm{r}}i_{\mathrm{r}q} + L_{\mathrm{o}}i_{sq}) - L_{\mathrm{o}}\frac{\mathrm{d}i_{sd}}{\mathrm{d}t}. \tag{11}$$

The developed electromagnetic torque T_{e} in *d-q* variables is given as

$$T_{\mathrm{e}} = \frac{3}{2}\left(\frac{p}{2}\right)L_{\mathrm{o}}(i_{sq}i_{\mathrm{r}d} - i_{sd}i_{\mathrm{r}q}). \tag{12}$$

The simulation model for studying the dynamic response of the system is developed using Eqs. (1)–(12).

4 Power flow control strategy

As mentioned earlier, a smooth coordinated control strategy between the diesel generator and BESS is essential for the optimum performance of hybrid autonomous power system (HAPS). Figure 2 shows the schematic block of the control circuit. A systematic and elaborate control is necessitated in the standalone power system. The speed, voltage and current signals from the synchronous generator, the grid and inverter are sensed and fed to the controller.

The error in speed is obtained by comparing the rotor speed with the reference speed and is given to a proportional controller that calculates the real current reference ($I_{d\mathrm{ref}} = I_{dd}$). If the diesel generator output is less than 40% of its rated capacity, the reference current ($I_{d\mathrm{ref}} = I_d$) is generated based on the speed of the generator and the difference between the actual ($I_{d\mathrm{act}}$) and set ($I_{d\mathrm{set}}$) value of diesel generator current.

The output power is controlled by controlling the $I_{d\mathrm{ref}}$ which in turn depends on I_d and I_{dd}.

$$I_{dd} = K_{\mathrm{pw}}(\omega_{\mathrm{ref}} - \omega_{\mathrm{act}}), \tag{13}$$

$$I_{d\mathrm{ref}} = I_{dd} + I_{d\mathrm{s}}. \tag{14}$$

The $I_{d\mathrm{ref}}$ obtained from Eq. (14) decides the amount of real power that needs to be injected or absorbed from the grid. The reference voltage V_{ref} is compared with the grid voltage V_{act} and this mismatch in voltage is the input to the

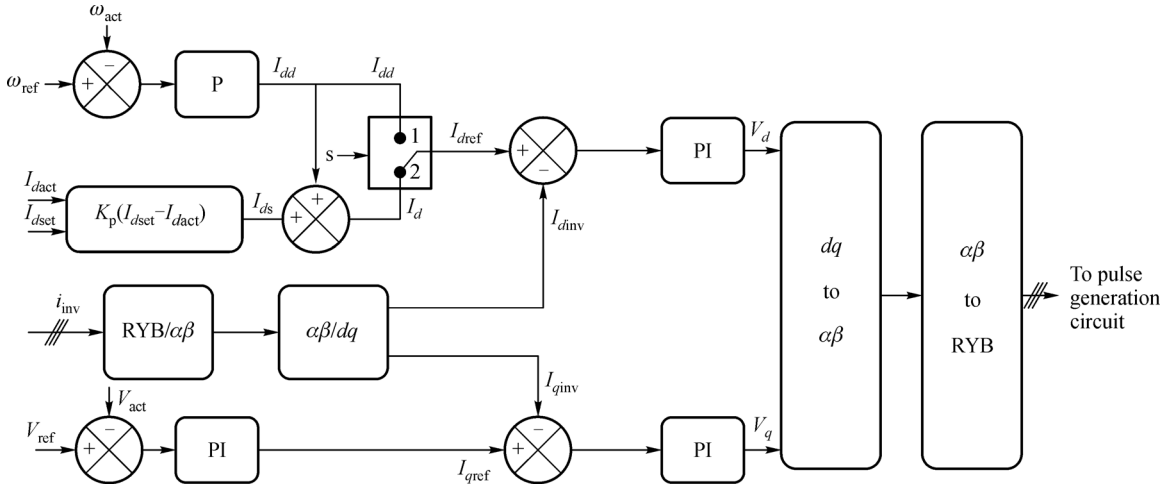

Fig. 2 Schematic diagram of the coordinated control strategy

proportional integral controller. The controller outputs a reactive current reference $I_{q\text{ref}}$ that can be used to control the reactive power that is absorbed from or injected into the grid.

$$I_{q\text{ref}} = K_{\text{pv}}(V_{\text{ref}} - V_{\text{act}}) + \frac{K_{\text{iv}}}{s}(V_{\text{ref}} - V_{\text{act}}). \quad (15)$$

The actual inverter current values in the *d-q* axes ($I_{d\text{inv}}$ and $I_{q\text{inv}}$) are compared with their respective reference quantities and are given as input to the PI controller. The K_{p} and K_{I} values are selected to make the closed loop system stable by using R-H criteria. The output of the controller is the control voltage in its respective *d-q* components which are then subsequently transformed to the *abc* axes. Further, the gate of inverter is driven by the signals obtained using the sinusoidal pulse width modulation technique using a carrier wave (frequency f_{c}) so as to synchronize this with the grid voltage.

5 Results and discussion

The performance of the control strategy is computed and tested in real time using Matlab/Simulink and time domain analysis is also performed. Further experiments are conducted on the laboratory prototype. The experimental setup is depicted in Fig. 3. An array of lead acid battery is used as a BESS. To increase the life of the battery, it operated in the range of 40% to 90% of state of charge (SOC). A storage battery is synchronized to the grid through a bidirectional converter (3 phase) which is essential for balancing the power in the grid. The line frequency transformer connects the diesel generator to the grid. The voltage and current transducers, LV25P and LA55P are used to sense the voltages (grid, battery) and current respectively. The bidirectional converter is constructed using SKM100GB 063D IGBTs and power diodes. A TMS320LF2407A DSP controller is used to execute the control strategy.

5.1 Standalone power system without BESS

The dynamic response of the power system is studied by applying a step change in load to the diesel generator.

5.1.1 Step increase in load

The system is modeled using Matlab/Simulink. Initially the system is subjected to a load of 2 kW. After $t = 12.5$ s, a step increase in load is made to 3 kW, thus stepping up by 1 kW. The speed of the diesel generator is decreased to 1445 r/min because of abrupt loading (Fig. 4(a)). The mechanical torque is increased to meet the load and the entire process consumes four seconds. The grid frequency is reduced to 48.16 Hz from 50 Hz as a result of the speed change. This has an impact on the sensitive loads connected in the grid (standalone).

The oscillations that are caused in the power output of the diesel and wind generator due the abrupt load change can be observed in Fig. 4(b). In the experiment, the speed of the synchronous generator falls to 1440 r/min with a settling time of 6 s. This causes the frequency to reduce to 48 Hz from 50 Hz (Fig. 4(c)), which clearly indicates that the deviation oversteps the IS: 1601:1960 standard limit, thus posing the threat of instability problem, which can be dominant when sensitive loads are connected.

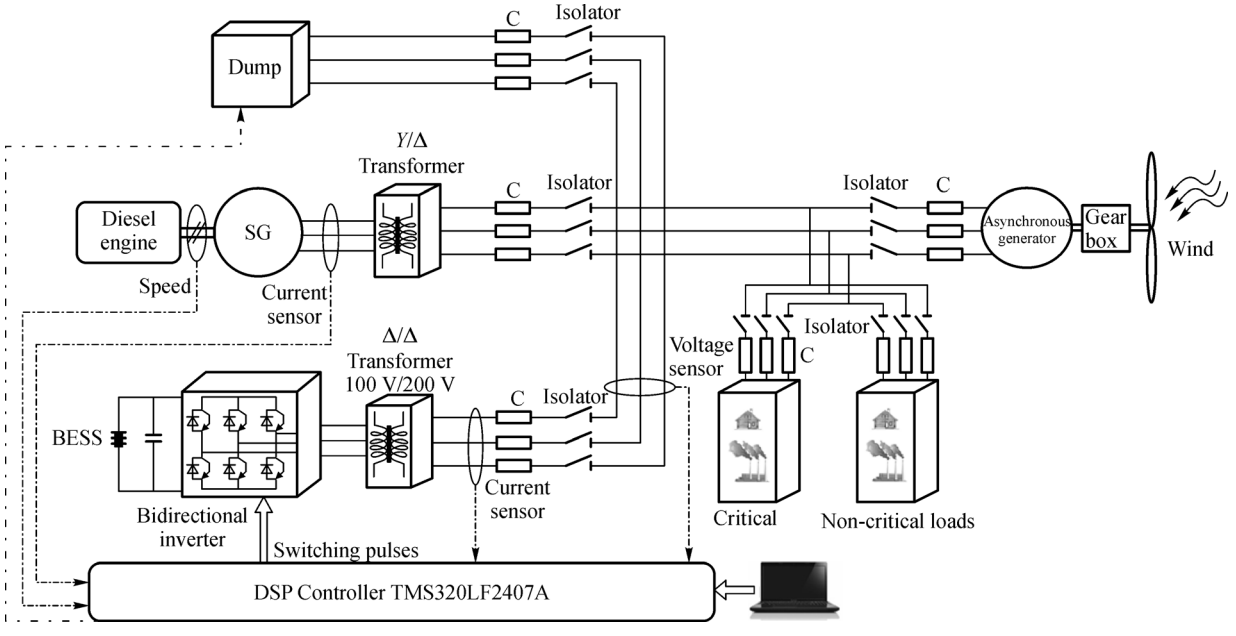

Fig. 3 Experimental setup of standalone power system

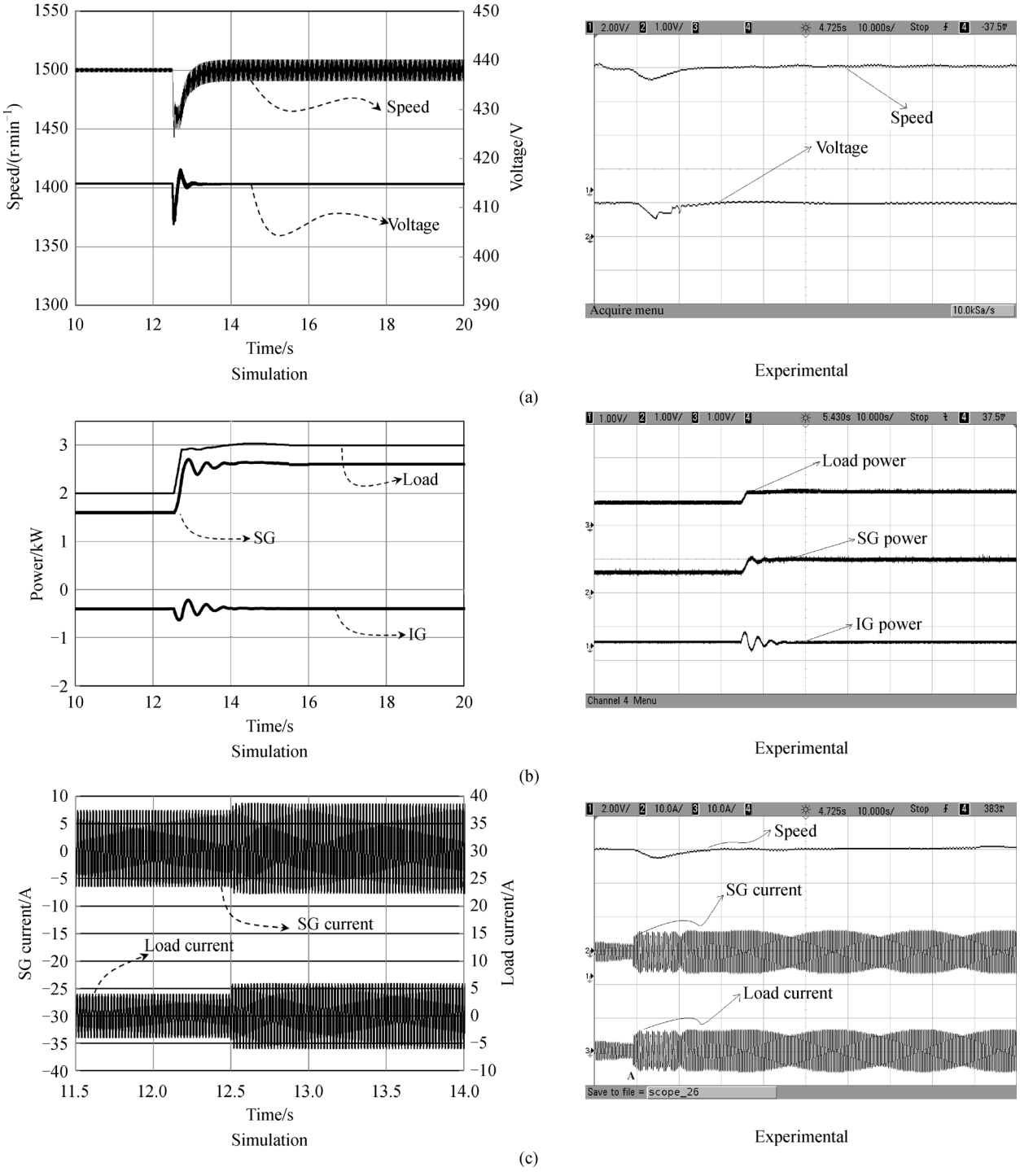

Fig. 4 Dynamic response for step increase in load (without BESS)
(a) Speed and voltage (Experimental scale (speed = 200 r/(min·div) (voltage = 415 V/div));
(b) power output (Experimental scale (power = 3000 W/div)); (c) current (Experimental scale (current = 10 A/div))

5.1.2 Step decrease in load

A step decrease of 1 kW is made at $t = 20$ s in simulation studies. The speed is increased to 1552 r/min from the prescribed 1500 r/min and the grid frequency increased to 51.7 Hz from the rated 50 Hz. This change can have a menacing impact on the sensitive loads in the power system. The variation of frequency and voltage is shown in Fig. 5 (a). The oscillations that are caused in the power output of the diesel and wind generator due the abrupt load change can be observed in Fig. 5 (b). Experiments on the laboratory setup demonstrate a similar response. The speed is increased to 1560 r/min and settles with a settling time of 8 s, thus changing the frequency to 52 Hz (Fig. 5(c)).

This clearly indicates that the deviation oversteps the IS: 1601:1960 standard limit and hence may have an adversely effect on the sensitive loads that are connected.

5.2 Standalone power system with BESS

A BESS is integrated into the system with the main objective of controlling the grid frequency within a set range. A smooth control strategy that controls the power flow between the synchronous generator and the BESS is incorporated. The dynamic response of the system is investigated and results obtained are presented.

5.2.1 Step increase in load

The simulation studies are performed after modeling the system with the proposed control strategy. The grid is driving a load of 2 kW and at $t = 12.5$ s instant, and a load of 1 kW is added (Fig. 6(b)). While loading, the diesel generator with a step change in the input, the BESS reacts quickly to inject the difference in power into the grid. This balances the power consumption and generation, thus gradually increasing the diesel generator output to meet the load demand over a duration of 7.5 s. Also, the rapid stress on the generator is prevented as shown in Fig. 6 (b). The speed of the generator is reduced to 1494 r/min in this case and the frequency is reduced to 49.8 Hz. Hence it can be observed that this change is viable as per the IS: 1601:1960 standards. Similar results that are obtained through experiments are depicted in Fig. 6 (c).

5.2.2 Step decrease in load

Simulation studies are conducted on the system to obtain the dynamic response under step decrease in load. The system is initially loaded to 3 kW and at $t = 20$ s, and the load is decreased by 1 kW. The speed of the diesel generator is increased to 1508 r/min (shown in Fig. 7(a)) and the bidirectional converter operates as a rectifier to store the surplus power in the battery (Fig. 7 (b)). During the load change, the synchronous generator is accelerated up to 1504 r/min and the frequency of the grid is increased to 50.13 Hz as observed in Fig. 7 (a). This satisfies the IS:1601:1960 standards. The experiments performed produce similar results and thus validate the performance of the scheme (Fig. 7 (c)). The frequency is increased to 50.26 Hz which is within the defined standard limits. It is notable from the results that the system shows a good dynamic response during load changes.

5.2.3 Under change in wind power and load

To analyze the effect of variation in wind power, the wind speed data of twelve hours is observed. Usually in autonomous power system, the variation in the grid power affects the grid frequency and voltage. Figure 8 displays the power output of the HAPS. In Fig. 8, the points *a*, *b* and *d* represent the variation in wind power and the points *c*, and *e* represent the change in load demand. For instance, the diesel generator supplies a power of 0.3 pu and the wind generator supplies a power of 0.2 pu to meet the load demand of 0.5 pu. At point *a*, the wind power is decreased to 0.18 pu. This sudden reduction in power generation is compensated by the battery for a short period of time and then gradually transferred to the diesel generator. Conversely, at point *b*, the wind power is increased from 0.18 pu to 0.21 pu. This increase in wind power is absorbed by the battery to balance the instantaneous power in the HAPS. Subsequently, this excess power absorbed by the battery is taken over by the diesel generator which leads to the reduction in diesel generator output power.

Similarly, the variation in load at points *c* and *d* is instantly compensated by the battery, and gradually these variations are absorbed by the diesel generator which enables the battery to operate in floating mode. Therefore, any load or wind power variations in the HAPS are instantly compensated by the battery, and gradually these variations are transferred to the diesel generator so that the grid voltage and frequency are maintained within the IS: 1601:1960 standard limits.

5.3 Dynamics during direct starting of induction machine

The dynamic response of the diesel generator is studied by connecting a 0.75 kW induction machine directly to the diesel generator at $t = 10$ s. The speed and frequency oscillate (48 Hz to 51.6 Hz) during the starting of the induction motor as noted from the simulation results (Fig. 9(a)).

This conspicuously exceeds the IS standards. The experimental results collude with the simulation results (Fig. 9 (b)). The dynamic behavior is also obtained when the BESS is connected to the grid (Fig. 9 (c) and 9(d)) and

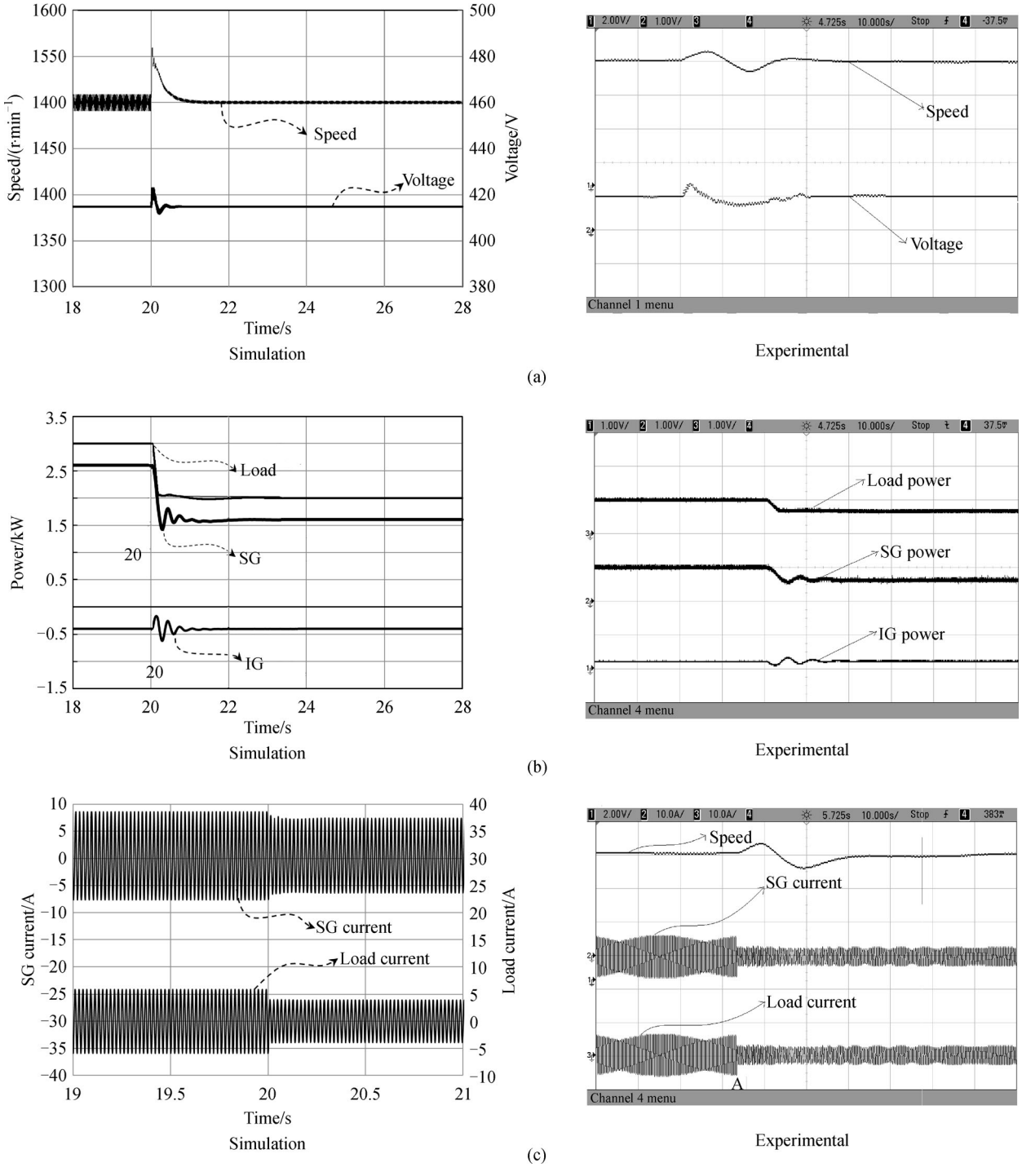

Fig. 5 Dynamic response for step decrease in load (without BESS)
(a) Speed and voltage (Experimental scale (speed = 200 r/(min·div) (voltage = 415 V/div));
(b) power output (Experimental scale (power = 3000 W/div)); (c) current (Experimental scale (current = 10 A/div))

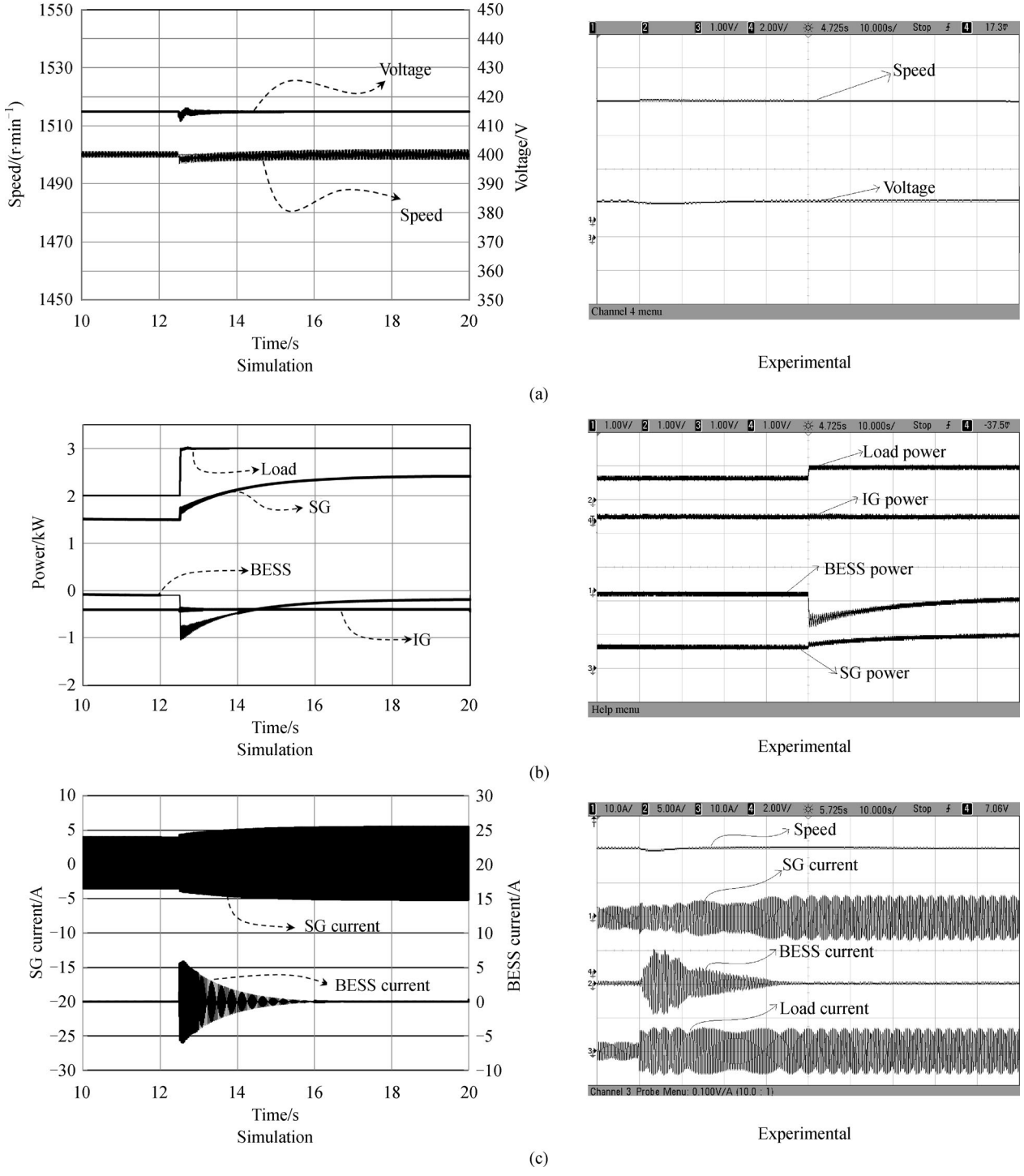

Fig. 6 Dynamic response for step increase in load with BESS
(a) Speed and voltage (Experimental scale (speed = 200 r/(min·div) (voltage = 415 V/div)); (b) power output (Experimental scale (power = 3000 W/div)); (c) current (Experimental scale SG current = 10 A/div, BESS current = 5 A/div, load current = 10 A/div)

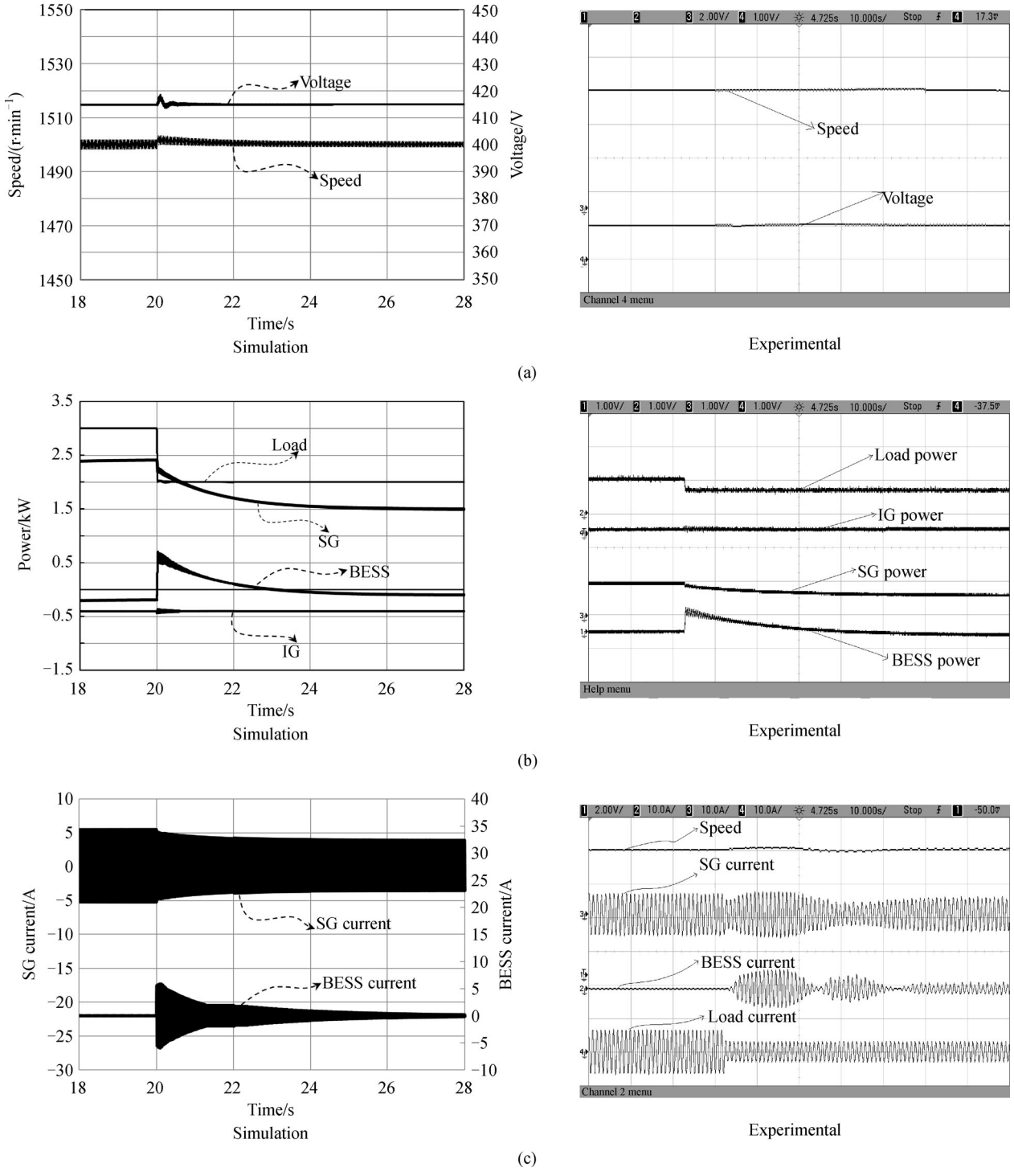

Fig. 7 Dynamic response for step decrease in load with BESS
(a) Speed and voltage (Experimental scale (speed = 200 r/(min·div) (voltage = 415V/div)); (b) power output (Experimental scale (power = 3000 W/div)); (c) current (Experimental scale SG current = 10 A/div, BESS current = 10 A/div, load current = 10 A/div)

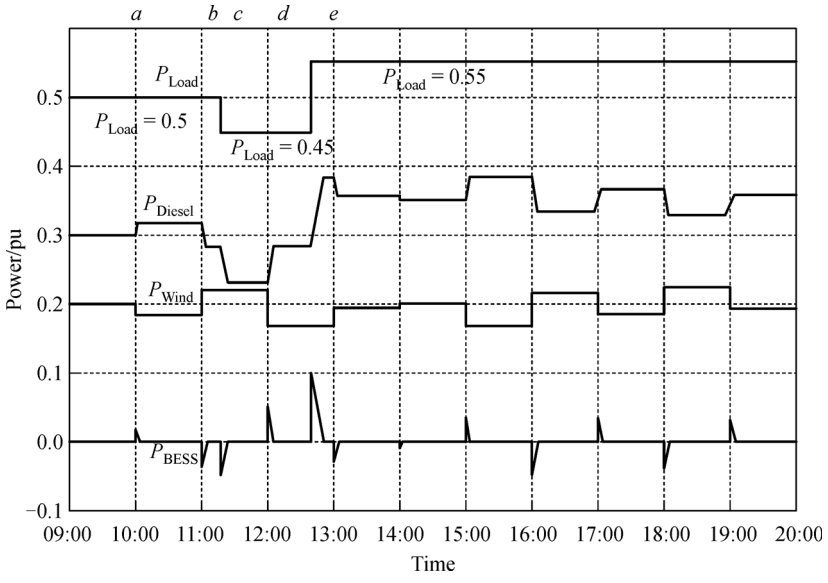

Fig. 8 Power output of HAPS under change in wind speed and load demand

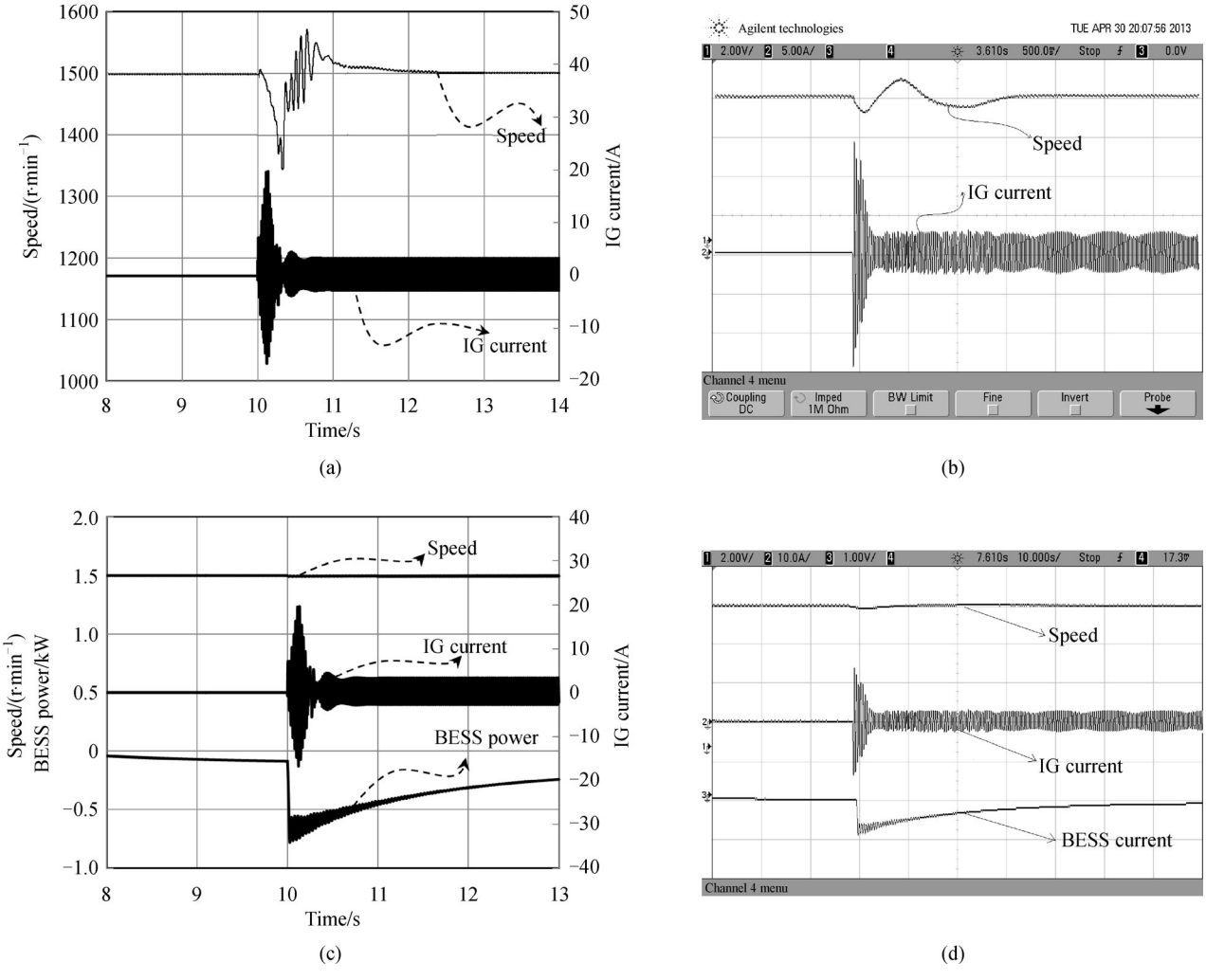

Fig. 9 Dynamic response during direct starting of induction machine (without BESS)
(a) Simulation (without BESS); (b) experimental (without BESS); (c) simulation (with BESS); (d) experimental (with BESS)

hence proves desirable. The required power is provided by the BESS, thus reducing the rapid stress on the DG and hence, attenuating the frequency oscillations.

6 Conclusions

A smooth coordinated control strategy for the harmonized operation of the BESS and diesel generator in a standalone power system was presented. The dynamic response characteristics were obtained through simulation as well as laboratory experiments and the results were presented. The practicability of this scheme was established and the performance was verified. The system performance was studied for step changes (increase and decrease) in load and for change in induction motor load. The system frequency obtained under these conditions is within the IS: 1601:1960 standard limits due to the smooth sharing of power between the DG and the BESS as enabled by the proposed coordinated control strategy. The algorithm for this strategy was implemented and executed on a TMS 320LF2407A DSP controller. The coherent results obtained through simulation and experiments validate the feasibility of the proposed system and control strategy.

Acknowledgements The authors wish to thank the authorities of the National Institute of Technology, Tiruchirappalli, India for all the facilities provided for carrying out the experimental and simulation work for the preparation of this paper. The authors also wish to thank NaMPET, an initiative of DIT, Govt. of India for providing fund for infrastructure development of Power Converters Research Laboratory, in which the experiments have been carried out.

Notations

v	Instantaneous voltage/V
i	Instantaneous current/A
V	Per-phase steady-state voltage (rms)/V
I	Per-phase steady-state current (rms)/A
R	Resistance/Ω
L	Inductance/H
P	Power/W
r_{sh}	Shunt resistance per phase/Ω
ω	Angular frequency (electrical)/(rad·s^{-1})
ω_e	Angular speed of rotor (electrical)/(rad·s^{-1})
L_{sh}	Shunt leakage inductance per phase/H
L_{md}	d-axis magnetizing inductance/H
L_{mq}	q-axis magnetizing inductance/H
L_{lfd}	field leakage inductance/H
λ	Flux linkage/Wb
K_p	Proportional gain
K_i	Integral gain

Subscripts

r	Rotor
s	Stator
m	Mutual
ls	Stator leakage
f	Field
p	Phase
t	Terminal
d	Direct axis
q	Quadrature axis
ref	Reference
inv	Inverter

Appendix

A1. Specifications of the synchronous machine:
3 Φ, 50 Hz, four-pole, 220 V, 3.8 A, 0.75 kW.
Machine parameters:
Stator resistance (R_s): 9.5 Ω/ph;
Rotor resistance (R_r): 12.08 Ω/ph;
Stator and rotor leakage reactance (Xl_s and Xl_r): 12 Ω/ph;
Moment of inertia: 0.02 kg·m^2.

A2. Specifications of the induction machine:
3 Φ, 50 Hz, four-pole, 220 V, 3.8 A, 3.7 kW.
Machine parameters:
Stator resistance (R_s): 2.7 Ω/ph;
Field resistance (R_f): 143.1 Ω;
Stator leakage reactance (Xl_s): 12.78 Ω/ph;
Rotor leakage reactance (Xl_r): 212.89 Ω;
Moment of inertia: 0.02 kg·m^2.

References

1. Rosas-Casals M. Power grids as complex networks: topology and fragility. In: Complexity in Engineering, 2010 (COMPENG '10). Rome, 2010, 21–26
2. Foley G. Rural electrification in the developing world. Energy Policy, 1992, 20(2): 145–152
3. Urmee T, Harries D, Schlapfer A. Issues related to rural electrification using renewable energy in developing countries of Asia and Pacific. Renewable Energy, 2009, 34(2): 354–357
4. Himri Y, Boudghene Stambouli A, Draoui B, Himri S. Techno-economical study of hybrid power system for a remote village in Algeria. Energy, 2008, 33(7): 1128–1136
5. Rehman S, El-Amin I M, Ahmad F, Shaahid S M, Al-Shehri A M, Bakhashwain J M, Shash A. Feasibility study of hybrid retrofits to an isolated off-grid diesel power plant. Renewable & Sustainable Energy Reviews, 2007, 11(4): 635–653
6. Payne M G. Motor starting on diesel generators. Electronics and Power, 1977, 23(6): 479–483
7. Chen Z, Hu Y. A hybrid generation system using variable speed

wind turbines and diesel units. The 29th Annual Conference of the IEEE Industrial Electronics Society, 2003, 3: 2729–2734

8. Lautier P, Prevost M, Ethier P, Martel P, Lavoie L. Off-grid diesel power plant efficiency optimization and integration of renewable energy sources. In: IEEE Canada Electrical Power Conference (EPC 2007). Montreal, 2007, 274–279
9. Bao N, Ma X, Ni W. Investigation on the integral output power model of a large-scale wind farm. Frontiers of Energy and Power Engineering in China, 2007, 1(1): 67–78
10. Chakraborty A. Advancements in power electronics and drives in interface with growing renewable energy resources. Renewable & Sustainable Energy Reviews, 2011, 15(4): 1816–1827
11. Chakraborty S, Kramer B, Kroposki B. A review of power electronics interfaces for distributed energy systems towards achieving low-cost modular design. Renewable & Sustainable Energy Reviews, 2009, 13(9): 2323–2335
12. Sharma H, Islam S, Pryor T, Nayar C V. Power quality issues in a wind turbine driven induction generator and diesel hybrid autonomous grid. Journal of Electrical and Electronics Engineering, Australia, 2001, 21(1): 19–25
13. Mahdad B, Srairi K. Solving multi-objective optimal power flow problem considering wind-STATCOM using differential evolution. Frontiers in Energy, 2013, 7(1): 75–89
14. Verma Y P, Kumar A. Load frequency control in deregulated power system with wind integrated system using fuzzy controller. Frontiers in Energy, 2013, 7(2): 245–254
15. Dai Y, Jiang P, Gao L, Kan W, Xiao X, Jin G. Capacity limitation of nuclear units in grid based on analysis of frequency regulation. Frontiers in Energy, 2012, 6(2): 148–154
16. Verma Y P, Kumar A. Dynamic contribution of variable-speed wind energy conversion system in system frequency regulation. Frontiers in Energy, 2012, 6(2): 184–192
17. Katsaprakakis D A, Christakis D G, Zervos A, Papantonis D, Voutsinas S. Pumped storage systems introduction in isolated power production systems. Renewable Energy, 2008, 33(3): 467–490
18. Kim Y M, Shin D G, Favrat D. Operating characteristics of constant-pressure compressed air energy storage (CAES) system combined with pumped hydro storage based on energy and exergy analysis. Energy, 2011, 36(10): 6220–6233
19. Basbous T, Younes R, Ilinca A, Perron J. Pneumatic hybridization of a diesel engine using compressed air storage for wind-diesel energy generation. Energy, 2012, 38(1): 264–275
20. Sebastian R. Modelling and simulation of a high penetration wind diesel system with battery energy storage. International Journal of Electrical Power & Energy Systems, 2011, 33(3): 767–774
21. Sebastián R, Peña Alzola R. Simulation of an isolated Wind Diesel System with battery energy storage. Electric Power Systems Research, 2011, 81(2): 677–686
22. Sebastián R. Reverse power management in a wind diesel system with a battery energy storage. International Journal of Electrical Power & Energy Systems, 2013, 44(1): 160–167
23. Sebastián R, Peña Alzola R. Effective active power control of a high penetration wind diesel system with a Ni–Cd battery energy storage. Renewable Energy, 2010, 35(5): 952–965
24. Cai Z, Ou X, Zhang Q, Zhang X. Full lifetime cost analysis of battery, plug-in hybrid and FCEVs in China in the near future. Frontiers in Energy, 2012, 6(2): 107–111
25. Stott P A, Mueller M A, Colli V D, Marignetti F, Di Stefano R. DC link voltage stabilisation in hybrid renewable diesel systems. In: International Conference on Clean Electrical Power, 2007 (ICCEP '07). Capri, 2007, 20–25
26. Xu L, Miao Z, Fan L. Coordinated control of a solar and battery system in a microgrid. In: 2012 IEEE PES Transmission and Distribution Conference and Exposition (T&D). Orlando, 2012, 1–7
27. Cha S T, Zhao H, Wu Q, Saleem A, Ostergaard J. Coordinated control scheme of battery energy storage system (BESS) and distributed generations (DGs) for electric distribution grid operation. In: 38th Annual Conference on IEEE Industrial Electronics Society (IECON 2012). Montreal, 2012, 4758–4764
28. Senjyu T, Kikunaga Y, Yona A, Sekine H, Saber A Y, Funabashi T. Coordinate control of wind turbine and battery in wind power generator system. In: 2008 IEEE Power and Energy Society General Meeting–Conversion and Delivery of Electrical Energy in the 21st Century. Pittsburgh, 2008, 1–7